



Spectral Analysis of Forbush Decreases Using a New Yield Function

M. Livada¹ · H. Mavromichalaki¹

Received: 14 April 2020 / Accepted: 30 July 2020 / Published online: 17 August 2020
© Springer Nature B.V. 2020

Abstract The Forbush decreases of the cosmic ray intensity observed on 24 December 2014 and on 8 September 2017 were chosen for cosmic ray spectral analysis. At first an analytical study of the solar and geomagnetic parameters of these events was carried out due to the fact that both are typical cosmic ray events. Hourly cosmic ray data of the neutron monitor stations obtained from the high-resolution neutron monitor database were used for calculating the cosmic ray density and anisotropy variations. Following the method of the coupling coefficients, the galactic cosmic ray spectral index was calculated using the technique of Wawrzynczak and Alania (Adv. Space Res. **45**, 622, 2010). A newly presented yield function by Mishev, Usoskin, and Kovaltsov (J. Geophys. Res. **118**, 2783, 2013) including a geometrical correction factor, already used in the spectral analysis of the cosmic ray ground level enhancements, was applied for the first time to the case of Forbush decreases. A comparison of these results during the events is performed by using two other coupling functions: the function presented in the work of Clem and Dorman (Space Sci. Rev. **93**, 335, 2000) and the one in the work of Belov and Struminsky (Proc. 25th Int. Cosmic Ray Conf. **1**, 201, 1997). The latter includes an extension for neutron monitor stations with rigidity $1 \text{ GV} < R < 2.78 \text{ GV}$. The obtained spectral index and the calculated cosmic ray intensity in the heliosphere during the two Forbush decreases after the coupling by these three functions are presented and discussed.

Keywords Galactic cosmic rays · Neutron monitors · Spectral analysis · Forbush decreases · Ground level enhancements

1. Introduction

Sharp reductions of the cosmic rays, observed followed by a gradual recovery lasting for 7–10 days, are defined as Forbush decreases (Fds). They were first noted by Forbush (1937)

✉ H. Mavromichalaki
emavromi@phys.uoa.gr

M. Livada
mairliv@phys.uoa.gr

¹ Faculty of Physics, National and Kapodistrian University of Athens, 15784 Athens, Greece

and Hess and Demmelmair (1937). These events are related to large solar flares and coronal mass ejections (CMEs) (Burlaga, 1995; Cane, 2000). An important feature of Fds when detected by neutron monitors is that their biggest decrease of the cosmic ray intensity in each station, defined as the amplitude of the Fd (%), is anticorrelated to the geomagnetic rigidity R (GV) of the galactic cosmic ray (GCR) particles (Smart et al., 2006). It is shown by Cane (2000) that it can be expressed by a power law $R^{-\gamma}$, where γ is the spectral index, that varies from ≈ 0.4 to 1.2. In fact, the spectral index values vary from ≈ 0.5 to 2 according to the method of Wawrzynczak and Alania (2010).

In the study of the galactic cosmic ray intensity, Dorman (1963) introduced the use of coupling functions with different parameters to be optimized. After parameterization of the results of Dorman and Yanke (1981) using altitude and rigidity dependencies, the function of Clem and Dorman (2000) was calculated. Now a days, due to the complexity of the atmospheric cascades, there are several yield functions and a Monte Carlo simulation is the most appropriate method for computing these functions. The FLUKtuierende KAskade (FLUKA) Monte Carlo package was used by Clem and Dorman (2000) for these simulations. The GEANT 4 Monte Carlo package was applied by Flückiger et al. (2008) and Matthiä et al. (2009) with the same aim. Recently, the GEANT 4 Planetocosmics Monte Carlo tool and a realistic atmospheric model were also used by Mishev, Usoskin, and Kovaltsov (2013) for the computations. The difference with this function is that for first time a geometrical factor, which provides a more extensive finite lateral contribution of the cosmic rays, is considered. In the lower energy range (< 10 GeV) the results of this yield function of Mishev, Usoskin, and Kovaltsov (2013) for protons are close to the computations by those functions of Flückiger et al. (2008) and Matthiä et al. (2009), who used the GEANT 4 Monte Carlo package, in contrast to those by Clem and Dorman (2000), which present discrepancies in this energy range. In the highest energy range (above 10 GeV) the new yield function gives greater values than all the others due to the rectification with the geometrical term of the neutron monitor (NM) effective region. According to Mishev, Usoskin, and Kovaltsov (2013), the results of the yield function corresponds better to the experimental latitude surveys of NMs. It is noted that till now it is not so easy to define the most appropriate yield function for the spectral calculations during various cosmic ray events.

In this work, we focus on the calculation of the cosmic ray spectral index during selected Fds applying the technique of Wawrzynczak and Alania (2010). Specifically, the coupling coefficient method that couples the cosmic ray intensity detected at ground-based stations to the cosmic ray flux in the free space was used for the calculation of the GCR spectrum. The daily values of the cosmic ray intensity in the heliosphere during the Fds, are calculated for various values of the spectral index in a particular range, applying the method of coupling coefficients. The values of the spectral index have to correspond to the values of the cosmic ray intensity in the heliosphere that are almost the same for all NMs, due to the fact that they are independent of the magnetic field. For the calculation of the spectral index values during such cosmic ray events, we attempt to find the most appropriate coupling function for the study of the cosmic ray spectrum (Yasue, Mori, and Sakakibara, 1982; Alania and Wawrzynczak, 2008).

Three different coupling functions were applied to the case of the above Forbush decreases of cosmic ray intensity to calculate the spectral index. The recently established yield function of Mishev, Usoskin, and Kovaltsov (2013) was used for the first time in Fds beyond the case of ground level enhancement (GLE) (Mishev et al., 2018; Koldobskiy et al., 2019).

The total response function of Clem and Dorman (2000) applied to polar and middle latitude neutron monitor stations and the function of Belov and Struminsky (1997) including

a separate term in $E^{3.17}$ to neutron monitor stations with rigidity between $1 \text{ GV} < R < 2.78 \text{ GV}$, were found to be suitable for the study of Fds. These two functions are suitable to apply in galactic and solar cosmic ray studies (Belov, Eroshenko, and Livshits, 1994; Belov and Eroshenko, 1996; Belov et al., 2005; Plainaki et al., 2007, 2014) for the NM64 and IGY type (developed during the International Geophysical Year, IGY) of neutron monitor stations with no significant variation (Clem and Dorman, 2000). In a previous work by Livada, Mavromichalaki, and Plainaki (2018) these two coupling functions were also applied for the calculation of the cosmic ray spectral index of the Fds of March 2012 with satisfactory results. In this work the use of the yield function of Mishev, Usoskin, and Kovaltsov (2013) also gives satisfactory results for the spectral index of the Fds, but only for sea-level neutron monitor stations. Its extension is important as it includes a geometric factor intrinsic of the neutron monitors which increases the sensitivity for high energy particles because of a lateral extent of the atmospheric cascade that is not provided by the previous coupling functions.

In this study, the Fd of December 2014–January 2015 that occurred after the maximum of Solar Cycle 24 and the Fd of September 2017 that occurred during the minimum of the same cycle, were selected for study applying the above-mentioned three different coupling functions. It is important to note that several X- and M-class solar flares and coronal mass ejections were caused on the Sun and created these two cosmic ray events. The goal of this work, besides using the coupling method, is to confirm the hypothesis that the calculated cosmic ray intensity in the heliosphere appears to be the same for all selected neutron monitors during the Fds and the calculated spectral index follows the structure of the events. A discussion of these results is presented.

2. Data Selection

For our study daily and 12-hourly cosmic ray data, corrected for pressure and efficiency of polar and mid latitude neutron monitors of the world wide network and obtained from the High-resolution real-time Neutron Monitor Database (NMDB) (<http://www.nmdb.eu>), were considered. The main characteristics of the stations used in this study including their cutoff rigidity are given in Table 1.

The cosmic ray intensity recorded at each station was normalized according to

$$J_i^k = \frac{N_k - N_0}{N_0} \quad (1)$$

where J_i^k is the normalized cosmic ray intensity for the i station of the Fd, N_k is the cosmic ray intensity of each station for k days or hours, and N_0 is the average cosmic ray intensity of three days before the beginning of the Fd (Wawrzynczak and Alania, 2010; Livada, Mavromichalaki, and Plainaki, 2018). The normalized ground-based intensity of cosmic rays for the selected stations from 21 December 2014–14 January 2015 (named Event-1) are presented in the upper panel of Figure 1 and from 7 to 12 September 2017 (named Event-2) in the lower panel of the same figure. It is noteworthy that in the recovery phase of the Fd of 8 September 2017, a ground level enhancement (GLE) on 10 September 2019 was recorded, identified as GLE72 (Mavromichalaki et al., 2018). The GLE72 was recorded by polar stations, such as Fort Smith and South Pole of the worldwide neutron monitor network provided by the NMDB. The Athens Neutron Monitor Station (A.Ne.Mo.S.) detected successfully the GLE72 in real time by the GLE Alert plus System (Mavromichalaki et al., 2018). Moreover, it is observed from Figure 1 that in both

Table 1 Characteristics of the neutron monitor stations used in this work.

NM stations	Abbr.	Detector type	Geographic coordinates	Altitude (m)	Cutoff rigidity (GV)
South Pole Antarctica	SOPO	3NM64	90.0° S N/A	2820	0.10
Fort Smith Canada	FSMT	18NM64	60.02°N 111.93°W	180.00	0.30
McMurdo Antarctica	MCMU	18NM64	77.9° S 166.6°E	48.00	0.30
Apatity Russia	APTY	18NM64	67.57°N 33.40°E	181.00	0.65
Oulu Finland	OULU	9NM64	65.05°N 25.47°E	15.00	0.81
Rome Italy	ROME	20NM64	41.86°N 12.47°E	Sea level	6.27
Guadalajara Spain	CALM	15NM64	40.33°N 3.9°W	708.00	6.95
Athens Greece	ATHN	6NM64	37.97° N 23.78° E	260.00	8.53

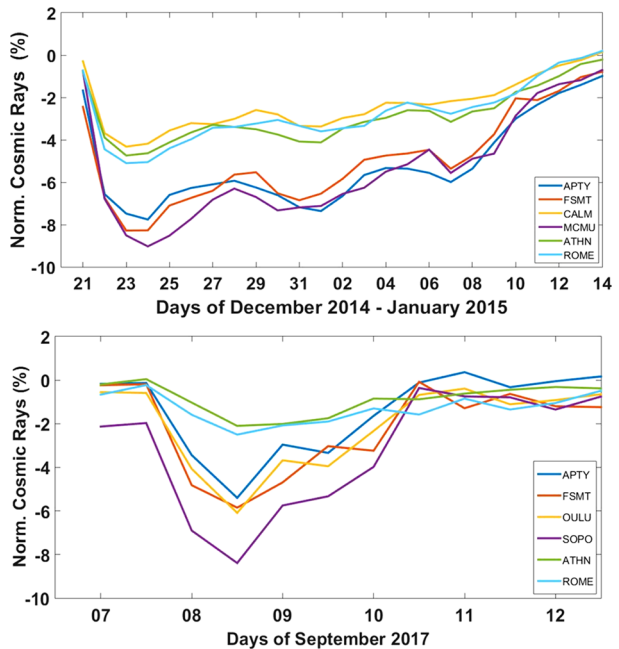
events the normalized cosmic ray intensity and the cutoff rigidity of each station are anti-correlated (Usoskin et al., 2008; Lingri et al., 2016). The normalized cosmic ray intensity presents smaller values in the mid latitude stations in contrast to the polar stations. It is well known that the dependence of the normalized cosmic ray intensity on the cutoff rigidity of each station can be expressed by an exponential dependence (Dorman et al., 2000; Caballero-Lopez and Moraal, 2012).

The solar characteristics of these Fds, such as M- and X-solar flares and halo CMEs associated with these events, were taken from the National Oceanic and Atmospheric Administration (NOAA) (<ftp.ngdc.noaa.gov>, <http://cdaw.gsfc.nasa.gov>, <http://umtof.umd.edu/pm/>, <https://www.solarmonitor.org/>, <https://kauai.ccmc.gsfc.nasa.gov/DONKI/>).

Specifically, Event-1 regarding solar activity occurred in the time period from 18 December 2014 till 14 January 2015 that is after the maximum of Solar Cycle 24 (Lingri et al., 2016). A number of 11 M-class flares and one X-class flare and a number of 6 CMEs took place on the Sun, as detected by GOES and the Large Angle and Spectrometric Coronagraph (LASCO) onboard the Solar and Heliospheric Observatory (SOHO) (<cdaw.gsfc.nasa.gov>, <http://umtof.umd.edu/pm/>). On 20 December 2014 an X1.8 flare and the accompanying CME with a velocity up to 830 km s⁻¹ were recorded. The solar active region (AR) 2242 (NOAA) with heliographic coordinates S18W29 was associated with this flare. As a result of this event, a Fd from 21 December 2014 till 14 January 2015 was recorded by the neutron monitors (<http://www.nmdb.eu>). The Fd amplitude occurred on 24 December 2014 with a value of -9.03% for the McMurdo neutron monitor station. Event-1 was interesting due to the fact that the recovery phase was very slow and complicated.

Concerning Event-2, during the time period of 6 to 10 September 2017, 23 M-class and 4 X-class flares and 3 CMEs took place, as detected with GOES and SOHO/LASCO instruments (<https://www.solarmonitor.org/>, <https://kauai.ccmc.gsfc.nasa.gov/DONKI/>). The solar event related to this Fd originated from the solar AR 2673 (NOAA). The Fd on 8 September 2017 was associated with two important solar flares. The first one was the X2.2 flare on 6 September 2017 followed by an X9.3 which were associated with a CME with velocity up to 1238 km s⁻¹. In addition, the Dst index on 8 September

Figure 1 Time profiles of the normalized CR intensity for polar and middle latitude neutron monitor stations obtained from the High-resolution Neutron Monitor Database (NMDB) for the period from 21 December 2014 till 14 January 2015 with daily data (upper panel) and for the period from 7 - 12 September 2017 with 12-hour data (lower panel).



2017 reached a minimum value of -142 nT and the Kp index had a maximum value of 8+ (<https://kauai.cmc.gsfc.nasa.gov/CMEScoreboard/>). The values of the geomagnetic indices and the great amplitude of the Fd on 8 September 2017 equal to 8.39% for the South Pole station, reveal an important geomagnetic storm (Mavromichalaki et al., 2018; Kurt et al., 2019).

3. Method of Analysis

The method described by Wawrzynczak and Alania (2010) and Alania and Wawrzynczak (2012) was also used in a previous work by Livada, Mavromichalaki, and Plainaki (2018) for the study of the event of March 2012, applying the two coupling functions (Clem and Dorman, 2000; Belov and Struminsky, 1997). In this new attempt the same method for the above selected Fds was used, applying in addition a new yield function (Mishev, Usoskin, and Kovaltsov, 2013) for the coupling in the heliosphere.

Concerning the Fd of December 2014 – January 2015 the cosmic ray intensity in the heliosphere and the spectral index were calculated using daily average cosmic ray data of six neutron monitors: Apatity (APTY), Fort Smith (FSMT), Guadalajara (CALM), McMurdo (MCMU), Athens (ATHN) and Rome (ROME). The Fd amplitude was recorded on 24 December 2014 (Figure 1). From this figure, it is obvious that there is a difference on the normalized cosmic ray intensity between the mid and the polar latitude stations. Specifically speaking, on 24 December 2014 the polar stations, recorded higher amplitudes, MCMU (9.03%) and FSMT (8.72%), in comparison to the mid latitude stations, such as ATHN (4.63%) and CALM (4.18%). This is due to the fact that the polar stations have smaller magnetic cutoff rigidity response to a larger energy range of the GCR spectrum. It is also significant to note that the ground-based cosmic ray intensity of the Fd depends also on the station altitude due to the atmospheric cascades.

Concerning the Fd of September 2017 the temporal changes of the rigidity spectrum were studied using 12-hour average corrected for pressure and efficiency of cosmic ray data by six neutron monitors: Apatity (APTY), Fort Smith (FSMT), Oulu (OULU), South Pole (SOPO), Athens (ATHN) and Rome (ROME)). For the calculations with the yield function of Mishev, Usoskin, and Kovaltsov (2013), the data of the SOPONM was not used in our analysis since this station is not a sea level one. For this Fd, the greater amplitude was observed on 8 September 2017 in the polar stations, as South Pole (8.39%), while in the mid latitude stations, as Athens, the amplitude was 2.1%.

According to Wawrzynczak and Alania (2010), for the study of the energy spectrum of the Fd, a method using functions which connect the cosmic rays of each neutron monitor station, depending on their local features with the primary cosmic rays in free space, is introduced.

Equation 2 represents the temporal intensity variations of GCRs during Fds as a power law in rigidity, where $\delta D(R)$ are the variations of the cosmic ray intensity, $R_0 = 1$ GV and $R_{max} = 200$ GV. R_{max} is the rigidity above which the Fd vanishes (Dorman, 2004).

$$\frac{\delta D(R)}{D(R)} = \begin{cases} A(\frac{R}{R_0})^{-\gamma} & R \leq R_{max} \\ 0 & R > R_{max} \end{cases} \tag{2}$$

In Equation 3 the average normalized cosmic ray intensity J_i^k of the Fds measured by the i neutron monitor for k days or hours, according to Equation 1 with respect to the geomagnetic cutoff rigidity R_i and the average atmospheric depth h_i , is determined. In this work the daily normalized cosmic ray intensity J_i^k of the first Fd and the 12-hourly normalized cosmic ray intensity of the second Fd for the i neutron monitor were calculated to be

$$J_i^k = \int_{R_i}^{R_{max}} (\frac{\delta D(R)}{D(R)})_k W_i(R_i, h_i) dR, \tag{3}$$

where $(\delta D(R)/D(R))_k$ is the rigidity spectrum of the Fd for the k day $W_i(R, h_i)$ is the coupling coefficient for the neutron or muon component of GCR and h is the atmospheric depth in bars (Dorman, 1963).

Finally, combining Equation 2 and 3, the normalized cosmic ray intensity of the Fd in the heliosphere A_i^k unaffected by the local features of the neutron or muon detector is given by

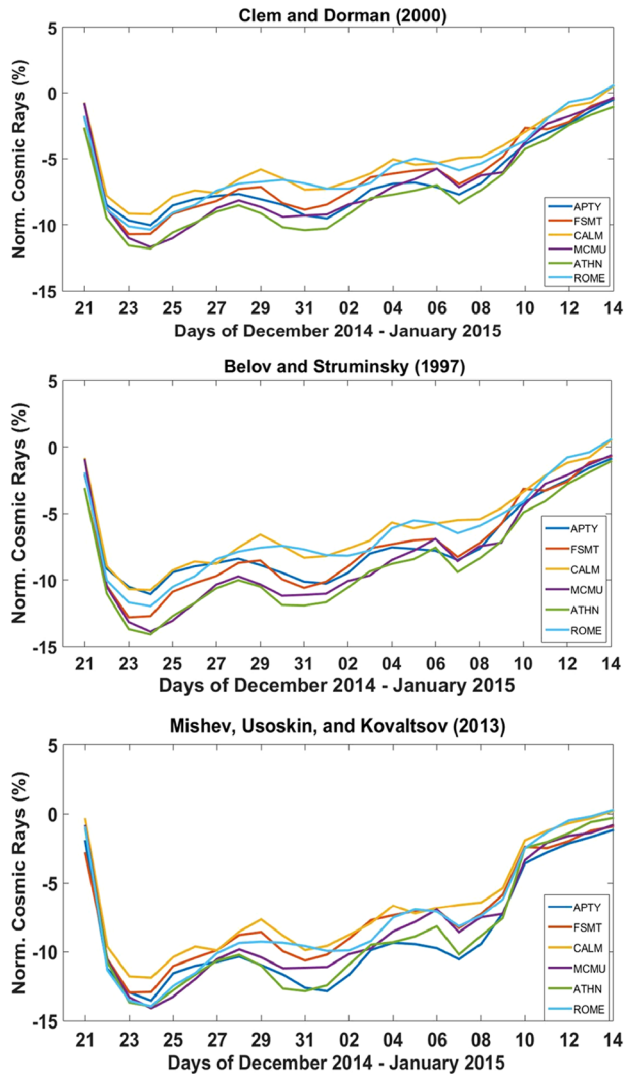
$$A_i^k = J_i^k / \int_{R_i}^{R_{max}} (\frac{R}{R_0})^{-\gamma} w_i(R_i, h_i) dR \tag{4}$$

In our analysis we calculated the cosmic ray intensity of the Fd in the heliosphere A_i^k (primary cosmic rays) according to Equation 4 for discrete values of γ ranging from 0.5 to 2 with a step of 0.01 using a Matlab program. So, the A_i^k was calculated for a series of 151 values of γ . The scheme of analysis was to select the most reliable value γ_0^k of each day, so the standard deviation according to Equation 5 was calculated also for a series of 151 values:

$$\sigma_\gamma^k = \sqrt{\sum_{i=1}^n (|A_i^k - \overline{A_i^k}|)^2 / (n - 1)}, \tag{5}$$

where $|A_i^k - \overline{A_i^k}|$ is considered as the difference between the mean $\overline{A_i^k}$ and the A_i^k cosmic ray intensity of the specific detector i and n is the number of neutron monitors.

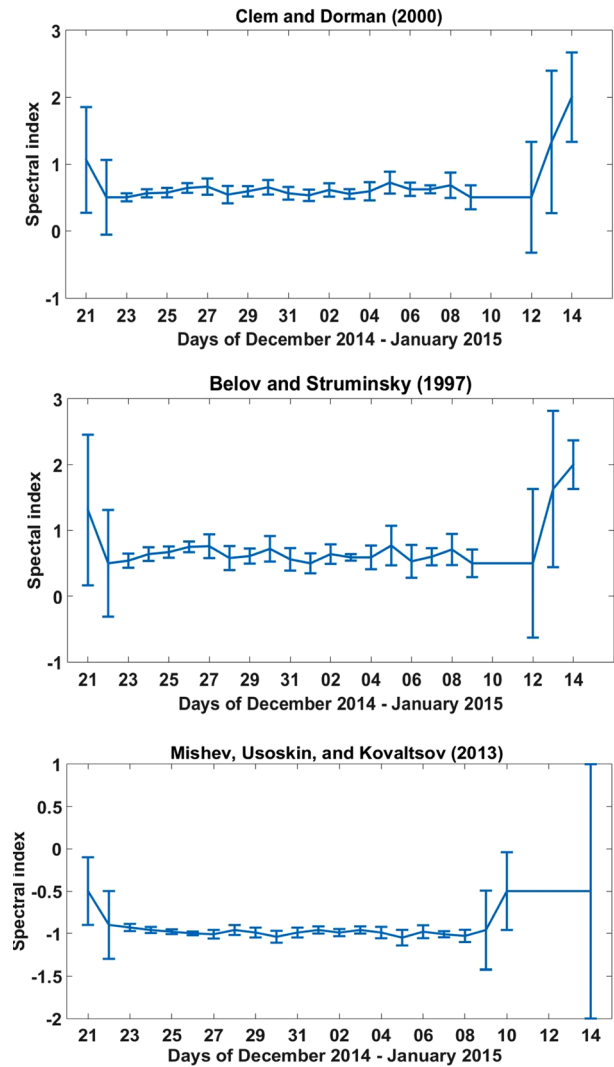
Figure 2 The calculated variations of the GCR intensity in the heliosphere recorded at the neutron monitor stations applying the coupling functions of Clem and Dorman (2000) (upper panel), Belov and Struminsky (1997) (middle panel) and Mishev, Usoskin, and Kovaltsov (2013) (lower panel) from 21 December 2014 till 14 January 2015 with daily data for polar and mid latitude neutron monitor stations.



The aim of this analysis is that the difference of the Fd of the cosmic ray intensity to be minimum $|A_t^k - \overline{A_t^k}|$ in order that A_t^k in free space to be the same for all selected neutron monitors. Then, an acceptable γ_0^k corresponds to a minimum value of the standard deviation. Finally to find the values of γ_0^k with a higher confidence level, two standard deviations have to be computed. For this purpose we calculated the error $\Delta\gamma$ of each γ_0^k , based on the previous (k-1) and the next value (k+1) of γ_0 (Alania and Wawrzynczak, 2008; Wawrzynczak and Alania, 2010).

Following this method, we computed the spectral index γ^k and the primary cosmic rays A_t^k in free space during the two different Fds of Solar Cycle 24. For the calculations three separated coupling functions were used and compared. It is noteworthy that one of these is a newly yield function which was used previously only in GLEs. The results of this analysis are given in Figures 2, 3 and 4, 5, respectively.

Figure 3 Temporal changes of the rigidity spectrum exponent from 21 December 2014 till 14 January 2015 calculated by the coupling functions of Clem and Dorman (2000), Belov and Struminsky (1997), and Mishev, Usoskin, and Kovaltsov (2013) in the upper, middle, and lower panels, respectively.



4. Coupling Functions and Results

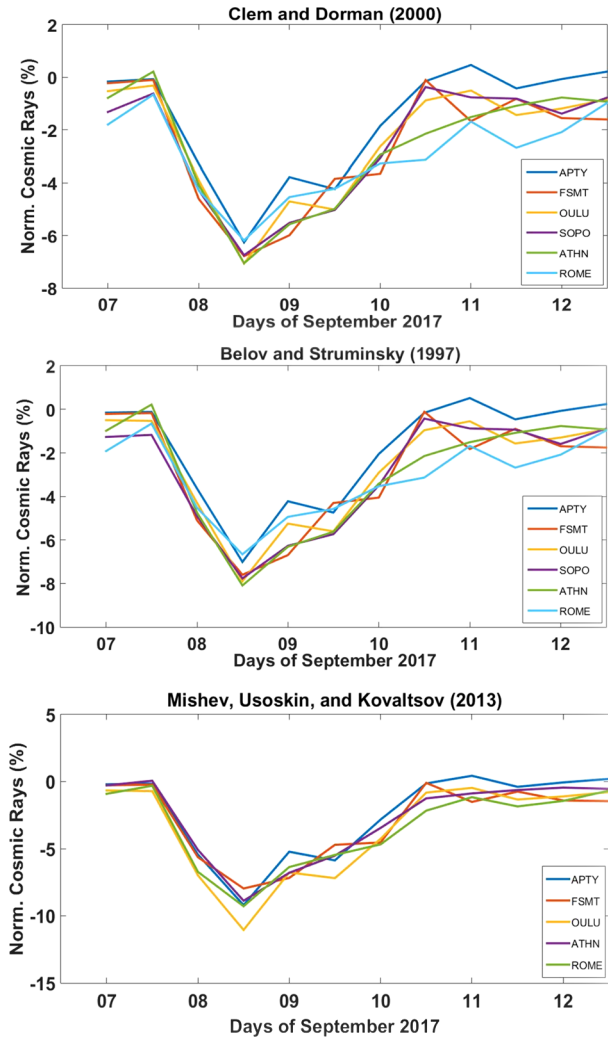
The above method was based on the coupling function $W_i(R_i h_i)$ between the normalized cosmic ray intensity of neutron monitors J_i^k and the primary cosmic rays A_i^k in free space that was determined from Equation 4. In this work we used and compared the results obtained using the three different coupling functions.

- i. The first coupling function is the total response function of Clem and Dorman (2000) given by

$$W(R_C) = \frac{-dN}{N(0)dR_C} = a(k-1)exp(-aR_C^{-K+1})R_C^{(-K)}, \tag{6}$$

where R_C is the cutoff rigidity of each station and α and κ are depth-dependent parameters which are determined by solar activity (minimum or maximum). This function and the pa-

Figure 4 The calculated variations of the GCR intensity in the heliosphere applying the coupling functions of Clem and Dorman (2000), Belov and Struminsky (1997), and Mishev, Usoskin, and Kovaltsov (2013) from 7 September till 12 September 2017 with 12-hour data from polar and mid latitude neutron monitor stations in the upper, middle, and lower panels respectively.



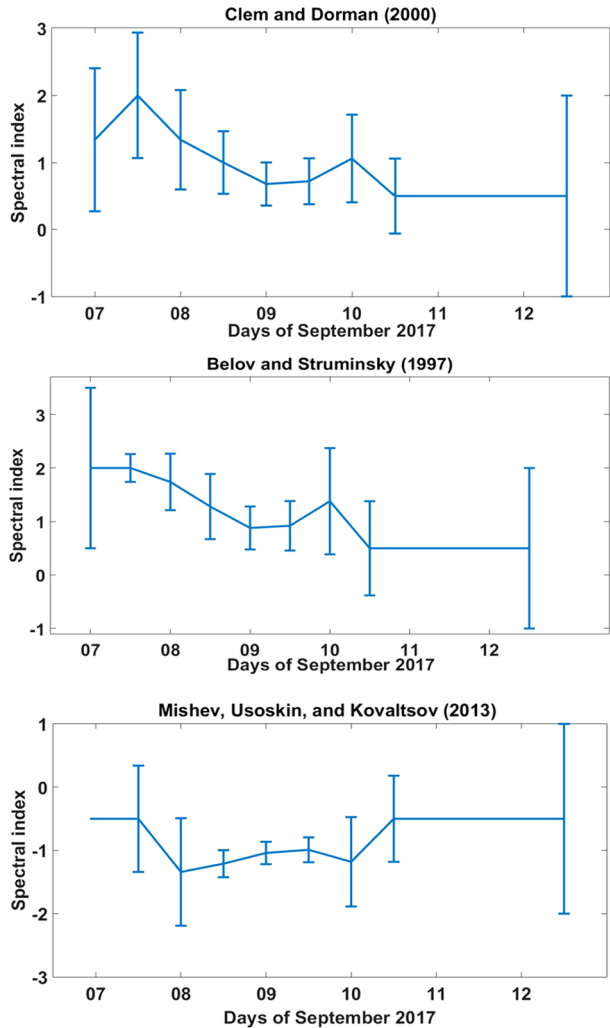
rameters α and κ respond better in the rigidity area of $2 \text{ GV} < R < 50 \text{ GV}$ (Dorman and Yanke, 1981), more details are given in Clem and Dorman (2000).

- ii. The second coupling function is related to the low kinetic energy range $1 \text{ GV} < E < 2.78 \text{ GV}$ and is described as a power law $\approx E^{3.17}$ given in Equation 7 (Belov and Struminsky, 1997; Plainaki et al., 2007, 2014).

$$W(R, h, t_0)dR = \begin{cases} W_T(R, h, t_0)dR, & R \geq 2.78 \text{ GV} \\ W(R = 2.78 \text{ GV}, h, t_0)\left(\frac{E}{2 \text{ GeV}}\right)^{3.17}dR, & R < 2.78 \text{ GV} \end{cases} \quad (7)$$

In our calculations the two coupling functions (Equations 6 and 7) were used for the polar neutron monitor stations with cutoff rigidity $R_c < 1 \text{ GV}$. This is not so significant, since 90% of the count rates of the polar neutron monitor stations are related to CRs above 5 GV (Maurin et al., 2015).

Figure 5 Temporal changes of the rigidity spectrum exponent γ applying the coupling function of Clem and Dorman (2000), Belov and Struminsky (1997), and Mishev, Usoskin, and Kovaltsov (2013) from 7 September till 12 September 2017 in the upper, middle, and lower panels, respectively.



iii. The third function is a newly computed yield function by Mishev, Usoskin, and Kovaltsov (2013). The neutron monitor yield function is defined (Flückiger et al., 2008) as:

$$Y_i(R, h) = \sum_j \iint A_i(E, \theta) F_{i,j}(R, h, E, \theta) dE d\Omega, \tag{8}$$

where $Y_i(R, h)$ in $m^2 sr$ is the NM yield function for primary particles of type i , R is the local geomagnetic cutoff rigidity, h is the atmospheric depth or altitude, $A_i(E, \theta)$ is the geometrical detector area related to the registration efficiency of the secondary particles (mainly neutrons and protons), $F_{i,j}$ is the differential flux of the secondary particles of type j (neutrons, protons, muons, and pions) for the primary particle of type i (protons), E is their secondary particle energy, θ is the angle of incidence. So, the yield function has the A term which is related to the response of the detector to secondary particles, and the F term which describes the atmospheric cascade of particles. The yield function was calculated for

the standard 6NM64 sea-level neutron monitors (Stoker, Dorman, and Clem, 2000; Moraal, Belov, and Clem, 2000). The GEANT 4 Planetocosmics Monte Carlo tool and the realistic model NRLMSISE2000 of the atmosphere were used for the calculations (Hatton, 1971; Picone et al., 2002; Agostinelli et al., 2003; Desorgher et al., 2005; Flückiger et al., 2008; Matthiä et al., 2009).

In the definition of the NM yield function of Mishev, Usoskin, and Kovaltsov (2013) except for the necessary computations, such as the Monte Carlo simulation, atmospheric models, and the response of the detector a new term for the effective area of the NM, the geometrical factor $G(R)$ was added (Equation 9). This term can correct the NM effective area which is mentioned to the finite lateral contribution of the cosmic rays and is slightly enhanced by the relative effects of higher energy particles (energy $> 5\text{-}10$ GeV/nucleon) in the NM count rate.

$$G(R) = \frac{2\pi}{S_{NM}} \int_0^\infty r w(r, R) dr, \quad (9)$$

where S_{NM} is the geometrical area of 6NM64, r is the distance from the center of the NM, $w(r, R)$ is the remote cascade; then the yield function (Equation 8) becomes

$$Y_i(R, h) = G(R) \sum_j \iint A_i(E, \theta) F_{i,j}(R, h, E, \theta) dE d\Omega. \quad (10)$$

A new computed yield function was presented in the work by Mishev, Usoskin, and Kovaltsov (2013) separately for primary CR protons and alpha particles for different energies. In this work the spectral analysis was defined by the computed yield function of Mishev, Usoskin, and Kovaltsov (2013) for CR protons of the standard 6NM64 sea-level neutron monitor for energies equal to 100 GV. Specifically the value was:

$$Y = 0.992 \text{ m}^2 \text{ sr}. \quad (11)$$

The yield function of Mishev, Usoskin, and Kovaltsov (2013) for protons, as provided by Maurin et al. (2015) is defined as:

$$I = \log_{10}(R) + 0.469$$

$$Y_p^{asl} = 10^{(-19.86 - 13.79I + 0.963I^2 + 30.56\sqrt{I})}. \quad (12)$$

The yield function of Mishev, Usoskin, and Kovaltsov (2013) (Equation 12) for protons, dependent on the cutoff rigidity R_c for the above Events-1 and -2, was studied. However, the results were not presented because this approach did not give us the expected ones, probably because it was not adapted to the method of Wawrzynczak and Alania (2010).

In this study, we applied the three above-mentioned coupling functions, using data for the selected neutron monitors in Table 1, for the calculation of the primary cosmic ray intensity and the spectral index during both Forbush decreases. We remark that in both cosmic ray events we did not use exactly the same stations due to their quality or data gaps. Concerning the calculated primary cosmic rays in the heliosphere according to the method of Wawrzynczak and Alania (2010), they are expected to be almost the same for all the selected mid and polar latitude stations since primary cosmic rays do not depend on the kind of detectors on Earth. In general, in all three functions used here, the above suggestion was confirmed with small discrepancies. In the case of Event-2 the coupling of the ground-based data with the primary ones seems to be better than in the case of Event-1 which means more

Table 2 Values of the spectral index for the time period 21 December 2014 till 14 January 2015.

Date YYYY/MM/DD	Clem and Dorman (2000)	Belov and Struminsky (1997)	Mishev, Usoskin, and Kovaltsov (2013)
2014/12/21	1.06 ± 0.79	1.31 ± 1.15	-0.50 ± 0.40
2014/12/22	0.50 ± 0.56	0.50 ± 0.81	-0.90 ± 0.40
2014/12/23	0.50 ± 0.06	0.54 ± 0.11	-0.93 ± 0.04
2014/12/24	0.56 ± 0.06	0.64 ± 0.10	-0.96 ± 0.04
2014/12/25	0.57 ± 0.07	0.67 ± 0.09	-0.98 ± 0.03
2014/12/26	0.64 ± 0.07	0.75 ± 0.08	-1.00 ± 0.02
2014/12/27	0.66 ± 0.12	0.76 ± 0.18	-1.01 ± 0.05
2014/12/28	0.54 ± 0.13	0.58 ± 0.18	-0.96 ± 0.06
2014/12/29	0.59 ± 0.08	0.61 ± 0.11	-0.99 ± 0.06
2014/12/30	0.65 ± 0.11	0.72 ± 0.19	-1.04 ± 0.07
2014/12/31	0.56 ± 0.09	0.56 ± 0.17	-0.99 ± 0.06
2015/01/01	0.53 ± 0.09	0.50 ± 0.15	-0.96 ± 0.04
2015/01/02	0.61 ± 0.10	0.64 ± 0.15	-0.99 ± 0.04
2015/01/03	0.55 ± 0.07	0.59 ± 0.05	-0.96 ± 0.04
2015/01/04	0.59 ± 0.14	0.59 ± 0.18	-0.99 ± 0.07
2015/01/05	0.72 ± 0.16	0.77 ± 0.30	-1.05 ± 0.09
2015/01/06	0.62 ± 0.10	0.53 ± 0.25	-0.98 ± 0.08
2015/01/07	0.62 ± 0.06	0.60 ± 0.13	-1.01 ± 0.04
2015/01/08	0.68 ± 0.19	0.71 ± 0.24	-1.03 ± 0.07
2015/01/09	0.50 ± 0.18	0.50 ± 0.21	-0.96 ± 0.47
2015/01/10	0.50 ± 0.00	0.50 ± 0.00	-0.50 ± 0.46
2015/01/11	0.50 ± 0.00	0.50 ± 0.00	-0.50 ± 0.00
2015/01/12	0.50 ± 0.83	0.50 ± 1.13	-0.50 ± 0.00
2015/01/13	1.33 ± 1.07	1.63 ± 1.19	-0.50 ± 0.00
2015/01/14	2.00 ± 0.67	2.00 ± 0.37	-0.50 ± 1.50

accurate and precise values of the expected spectral index. We think that possibly this difference is dependent on the structure and the long duration of the recovery phase of Event-2. This is well observed in Figures 2 and 4.

Following the above described technique we calculated the values of spectral index for the two events given in Tables 2 and 3 and presented in Figures 3 and 5, respectively. The error $\Delta\gamma$ of each spectral index was calculated based on their previous and following values. Thus, the calculated error of the spectral index appeared as $\Delta\gamma = 0$ (Tables 2 and 3) because the cosmic rays and the spectral index are stabilized. We notice here that the values of the spectral index are taken with a positive sign in the cases of the coupling functions given by Equations 6 and 7, while in the case of the coupling function given by Equation 10 (Mishev, Usoskin, and Kovaltsov, 2013) the values of γ have been taken with a negative sign. This was required for our results to be consistent with Figures 2-5 (Wawrzynczak and Alania, 2010; Mishev, Usoskin, and Kovaltsov, 2013).

Concerning the comparison of the function of Clem and Dorman (2000) with the function of Belov and Struminsky (1997), the differences were not important in any of the events, as they are coming only from the power law close to $E^{3.17}$ for the low kinetic energy, which is included in the function of Belov and Struminsky (1997). This term is not significant for the

Table 3 Values of the spectral index for the time period 7–12 September 2017.

Date YYYY/MM/DD hh:mm (UT)	Clem and Dorman (2000)	Belov and Struminsky (1997)	Mishev, Usoskin, and Kovaltsov (2013)
2017/09/07 00:00	1.34 ± 1.07	2.00 ± 1.50	-0.50 ± 0.00
2017/09/07 12:00	2.00 ± 0.93	2.00 ± 0.26	-0.50 ± 0.84
2017/09/08 00:00	1.34 ± 0.74	1.74 ± 0.53	-1.34 ± 0.85
2017/09/08 12:00	1.00 ± 0.47	1.28 ± 0.60	-1.21 ± 0.21
2017/09/09 00:00	0.68 ± 0.32	0.88 ± 0.40	-1.04 ± 0.17
2017/09/09 12:00	0.72 ± 0.34	0.92 ± 0.46	-0.99 ± 0.19
2017/09/10 00:00	1.06 ± 0.65	1.38 ± 0.99	-1.18 ± 0.71
2017/09/10 12:00	0.50 ± 0.56	0.50 ± 0.88	-0.50 ± 0.68
2017/09/11 00:00	0.50 ± 0.00	0.50 ± 0.00	-0.50 ± 0.00
2017/09/11 12:00	0.50 ± 0.00	0.50 ± 0.00	-0.50 ± 0.00
2017/09/12 00:00	0.50 ± 0.00	0.50 ± 0.00	-0.50 ± 0.00
2017/09/12 12:00	0.50 ± 1.50	0.50 ± 1.50	-0.50 ± 1.50

galactic cosmic rays, but only for the solar cosmic rays (GLEs). Finally, the yield function of Mishev, Usoskin, and Kovaltsov (2013) is a more strict function formalism in comparison to the two other coupling functions, which approached the registration efficiency of the secondary particles from the detectors and the effect of the flux of the secondary particles from the primary spectrum, nevertheless in this work the results were exported for a given cutoff rigidity.

5. Discussion and Conclusions

From the above analysis we conclude that:

- i. As it has already been established, there is a close relation of the cosmic ray intensity of the Fds recorded by the ground-based neutron monitor stations with the solar activity (Shrivastava, 2005). In the first studied Event-1, the amplitude of the Fd occurred on 24 December 2014 after an X-class flare on 20 December 2014 and a corresponding CME with velocity up to 830 km s^{-1} (Figure 1). For the second Event-2 according to Figure 1, the solar activity on 6 September 2017, specifically the X2.2 flare and the X.9.3 flare associated with a CME with velocity up to 1238 km s^{-1} , corresponds to the great amplitude of the Event-2 that occurred on 8 September 2017.
- ii. Moreover it was observed that, for both Fds when there is an increase in the cutoff rigidity R_c of the selected stations (mid latitude stations), the amplitude of the Fd diminishes (Figure 1). In previous work concerning the Fds, such as during the event of March 2012, the anticorrelation between the amplitude and the cutoff rigidity of each station was also appeared (Usoskin et al., 2008; Lingri et al., 2016; Livada, Mavromichalaki, and Plainaki, 2018). Specifically, the dependence of the cosmic ray intensity on the cutoff rigidity of each station can be expressed by an exponential and an anticorrelated dependence (Dorman et al., 2000; Caballero-Lopez and Moraal, 2012).

- iii. A cosmic ray spectral analysis in the two cases of Fds was performed by the method of Wawrzynczak and Alania (2010) and Alania and Wawrzynczak (2012) using three different coupling functions. The first one is the function of Clem and Dorman (2000), the second one is the function of Belov and Struminsky (1997) concerning stations with cutoff rigidity $R_c < 2.78$ GV, and the third one is the yield function of Mishev, Usoskin, and Kovaltsov (2013). It must be noted that the yield function of Mishev, Usoskin, and Kovaltsov (2013) is a newly computed function which includes a correction of a geometrical factor which is the neutron monitor effective area, suitable only for sea-level neutron monitor stations in comparison to the two other functions, which can be applied to every station irrespective of their heights. It has been applied till now only in the case of GLEs and not in the case of Fds.
- iv. According to the technique of Wawrzynczak and Alania (2010) and Alania and Wawrzynczak (2012) for reliable calculations of the spectral index values, it is suggested that the cosmic ray intensity in the free space A_1^k should be almost the same for all selected neutron monitors. It is noteworthy that the calculated cosmic ray intensity in the heliosphere by the three coupling functions seems to be almost the same for all stations in the two cases of Fds (Figures 2 and 4). There are some small differences between polar and mid latitude stations in the case of the Fd of September 2017 that means a more reliable calculated spectral index.
- v. The purpose of this work is to show that a characteristic of the calculated spectral index is to follow well the cosmic ray intensity during the Forbush decreases. The spectral index decreases in the minimum and near minimum phases of the Fd meaning the hardening of the rigidity spectrum due to the interplanetary magnetic structures before the beginning of the Fd event, which reflect the galactic particles of the lower energy. The results found for the spectral index with the above-mentioned coupling functions confirm this purpose, while the calculations by Mishev, Usoskin, and Kovaltsov (2013) function have been done only for a given rigidity.
- vi. Finally, the results of the calculated spectral index in both cases using the Fds by three coupling functions are also in agreement with the results of the events of September 2005 (Wawrzynczak and Alania, 2010), August 2010 (Livada, Papaioannou, and Mavromichalaki, 2013), March 2012 (Livada, Mavromichalaki, and Plainaki, 2018) etc., for which the two first coupling functions have been used. In these events the spectral exponent reached its biggest value at the beginning of the Fd and the minimum one at the main phase when the amplitude of the Fd was the biggest. It shows that the spectral exponent fluctuates accordingly to the structure of the Fd.
- vii. Summarizing, we can say that the new yield function of Mishev, Usoskin, and Kovaltsov (2013) provides a strict formalism in which the calculations have been done using the Monte Carlo tool, the realistic model of the atmosphere, and the geometrical correction of the NM effective area. When this function is based on the cutoff rigidity of each station it is not probably suitable for the analysis method used here. A future work including more events and possibly other yield functions will be very useful for space weather studies and applications.

Acknowledgements Many thanks are due to our collaborators of the neutron monitor stations for kindly providing the cosmic ray data used in this work from the High-resolution real-time Neutron Monitor database (NMDB), funded under the European Union FP7 Program (contract no. 213007). A.Ne.Mo.S. is supported by the Special Research Account of the National and Kapodistrian University of Athens. Thanks are also due to the editor and the anonymous referee of the Solar Physics for useful suggestions.

Disclosure of Potential Conflicts of Interest The authors declare that there is not conflict of interest.

Publisher's Note Springer Nature remains neutral with regard to jurisdictional claims in published maps and institutional affiliations.

References

- Agostinelli, S., Allison, J., Amako, K., Apostolakis, J., Araujo, H., Arce, P., et al.: 2003, GEANT4 a simulation toolkit. *Nucl. Instrum. Methods Phys. Res. A* **506**, 250. DOI.
- Alania, M.V., Wawrzynczak, A.: 2008, Forbush decrease of the galactic cosmic ray intensity: experimental study and theoretical modeling. *Astrophys. Space Sci. Trans.* **4**, 59. DOI.
- Alania, M., Wawrzynczak, A.: 2012, Energy dependence of the rigidity spectrum of Forbush decrease of galactic cosmic ray intensity. *Adv. Space Res.* **50**, 725. DOI.
- Belov, A.V., Eroshenko, E.A.: 1996, The energy spectra and other properties of the great proton events during 22nd solar cycle. *Adv. Space Res.* **17**, 167.
- Belov, A.V., Struminsky, A.B.: 1997, Neutron monitor sensitivity to primary protons below 3 GeV derived from data of ground level events. *Proc. 25th Int. Cosmic Ray Conf.* **1**, 201.
- Belov, A.V., Eroshenko, E.A., Livshits, M.A.: 1994, The energy spectra of the accelerated particles near the Earth and in the source in 15 June 1991 enhancement. *Proc. 8th Intern. Symp. on Solar Terrestrial Physics Pt. 1*, 26.
- Belov, A., Eroshenko, E., Mavromichalaki, H., Plainaki, C., Yanke, V.: 2005, Solar cosmic rays during the extremely high ground level enhancement on 23 February 1956. *Ann. Geophys.* **23**, 2281. DOI.
- Burlaga, L.F.: 1995, *Interplanetary Magnetohydrodynamics*, Oxford University Press, New York.
- Caballero-Lopez, R.A., Moraal, H.: 2012, Cosmic-ray yield and response functions in the atmosphere. *J. Geophys. Res.* **117**, A12. DOI.
- Cane, H.V.: 2000, Coronal mass ejections and Forbush decreases. *Space Sci. Rev.* **93**, 55. DOI.
- Clem, J., Dorman, L.: 2000, Neutron monitor response functions. *Space Sci. Rev.* **93**, 335. DOI.
- Desorgher, L., Flückiger, E.O., Gurtner, M., Moser, M.R., Bütikofer, R.: 2005, Atmocosmics: a Geant 4 code for computing the interaction of cosmic rays with the Earth's atmosphere. *Int. J. Mod. Phys. A* **20**, 6802. DOI.
- Dorman, L.I.: 1963, *Cosmic Rays Variations and Space Exploration*, Nauka, Moscow.
- Dorman, L.I.: 2004, *Cosmic Rays in the Earth's Atmosphere and Underground*, Kluwer, Dordrecht.
- Dorman, L.I., Yanke, V.: 1981, The coupling functions of NM-64 neutron super monitor. *Proc. 17th Int. Cosmic Ray Conf.* **4**, 326.
- Dorman, L.I., Villorei, G., Iucci, N., Parisi, M., Tyasto, M.I., Danilova, O.A., Ptitsyna, N.G.: 2000, Cosmic ray survey to Antarctica and coupling functions for neutron component near solar minimum (1996-1997) 3. Geomagnetic effects and coupling functions. *J. Geophys. Res.* **105**, 21047. DOI.
- Flückiger, E.O., Moser, M.R., Pirard, B., Bütikofer, R., Desorgher, L.: 2008, A parameterized neutron monitor yield function for space weather applications. In: Caballero, R., D'Olivo, J., Medina-Tanco, G., Nellen, L., Sánchez, F., Valdés-Galicia, J. (eds.) *Proc. 30th Intern. Cosmic Ray Conf.* **1**, 289.
- Forbush, S.: 1937, On the effects in cosmic-ray intensity observed during the recent magnetic storm. *Phys. Rev.* **51**, 1108. DOI.
- Hatton, C.J.: 1971, The neutron monitor. In: Wilson, J.G., Wouthuysen, S.A. (eds.) *Processes in Elementary Particle and Cosmic Ray Physics*, North-Holland, Amsterdam, 3.
- Hess, V.F., Demmelmair, A.: 1937, World-wide effect in cosmic ray intensity, as observed during a recent magnetic storm. *Nature* **140**, 316. DOI.
- Koldobskiy, S.A., Kovaltsov, G.A., Mishev, A.L., Usoskin, I.G.: 2019, New method of assessment of the integral fluence of solar energetic (> 1 GV rigidity) particles from neutron monitor data. *Solar Phys.* **294**(7), 18. DOI.
- Kurt, V., Belov, A., Kudela, K., Mavromichalaki, H., Kashapova, L., Yushkov, B., Sgouropoulos, C.: 2019, Onset time of the GLE 72 observed at neutron monitors and its relation to electromagnetic emissions. *Solar Phys.* **294**(22), 18. DOI.
- Lingri, D., Mavromichalaki, H., Belov, A., Eroshenko, E., Yanke, V., Abunin, A., Abunina, M.: 2016, Solar activity parameters and associated Forbush decreases during the minimum between cycles 23 and 24 and the ascending phase of cycle 24. *Solar Phys.* **291**, 1025. DOI.
- Livada, M., Papaioannou, A., Mavromichalaki, H.: 2013, Galactic cosmic ray spectrum and effective radiation doses on flights during Forbush decreases. *Proc. 11th HelAS Conf.*, S1-22.
- Livada, M., Mavromichalaki, H., Plainaki, C.: 2018, Galactic cosmic ray spectral index: the case of Forbush decreases of March 2012. *Astrophys. Space Sci.* **363**, 8. DOI.
- Matthiä, D., Heber, B., Reitz, G., Meier, M., Sihver, L., Berger, T., Herbst, K.: 2009, Temporal and spatial evolution of the solar energetic particle event on 20 January 2005 and resulting radiation doses in aviation. *J. Geophys. Res.* **114**, A08104. DOI.

- Maurin, D., Cheminet, A., Derome, L., Ghelfi, A., Hubert, G.: 2015, Neutron monitors and muon detectors for solar modulation studies: interstellar flux, yield function, and assessment of critical parameters in count rate calculations. *Adv. Space Res.* **55**, 363. [DOI](#).
- Mavromichalaki, H., Gerontidou, M., Paschalis, P., Paouris, E., Tezari, A., Sgouropoulos, C., Crosby, N., Dierckxsens, M.: 2018, Real-time detection of the ground level enhancement on 10 September 2017 by A.Ne.Mo.S.: System report. *Space Weather* **16**, 1797. [DOI](#).
- Mishev, A.L., Usoskin, I.G., Kovaltsov, G.A.: 2013, Neutron monitor yield function: new improved computations. *J. Geophys. Res.* **118**, 2783. [DOI](#).
- Mishev, A., Usoskin, I., Raukunen, O., Paassilta, M., Valtonen, E., Kocharov, L., Vainio, R.: 2018, First analysis of ground-level enhancement GLE72 on 10 September 2017: spectral and anisotropy characteristics. *Solar Phys.* **293**, 136. [DOI](#).
- Moraal, H., Belov, A., Clem, J.M.: 2000, Design and co-ordination of multi-station international neutron monitor networks. *Space Sci. Rev.* **93**, 285. [DOI](#).
- Picone, J.M., Hedin, A.E., Drob, D.P., Aikin, A.C.: 2002, NRLMSISE-00 empirical model of the atmosphere: Statistical comparisons and scientific issues. *J. Geophys. Res.* **107**(A12), 1468. [DOI](#).
- Plainaki, C., Belov, A., Eroshenko, E., Mavromichalaki, H., Yanke, V.: 2007, Modeling ground level enhancements: Event of 20 January 2005. *J. Geophys. Res.* **112**, A04102. [DOI](#).
- Plainaki, C., Mavromichalaki, H., Laurenza, M., Gerontidou, M., Kanellakopoulos, A., Storini, M.: 2014, The ground level enhancement of 2012 May 17: derivation of solar proton event properties through the application of the NMBANGLE PPOLA model. *Astrophys. J.* **785**, 160. [DOI](#).
- Shrivastava, P.: 2005, Study of large solar flares in association with halo coronal mass ejections and their helio-longitudinal association with Forbush decreases of the cosmic rays. *Proc. 29th Intern. Cosmic Ray Conf.* **1**, 355.
- Smart, D.F., Shea, M.A., Tylka, A.J., Boberg, P.R.: 2006, A geomagnetic cutoff rigidity interpolation tool: Accuracy verification and application to space weather. *Adv. Space Res.* **37**, 1206. [DOI](#).
- Stoker, P.H., Dorman, L.I., Clem, J.M.: 2000, Neutron monitor design improvements. *Space Sci. Rev.* **93**, 361. [DOI](#).
- Usoskin, I.G., Braun, I., Gladysheva, O.G., Horandel, J.R., Jamsen, T., Kovaltsov, G.A., Starodubtsev, S.A.: 2008, Forbush decreases of cosmic rays: Energy dependence of the recovery phase. *J. Geophys. Res.* **113**, A07102. [DOI](#).
- Wawrzynczak, A., Alania, M.: 2010, Modeling and data analysis of a Forbush decrease. *Adv. Space Res.* **45**, 622. [DOI](#).
- Yasue, S., Mori, S., Sakakibara, S.: 1982, Coupling coefficients of cosmic rays daily variations for neutron monitor stations. *Rep. Cosmic Ray Res. Lab.* **7**, Nagoya Univ.